Experimental and Theoretical Study of Deviations from Vegard's Law in the Sn_xGe_{1-x} System

A. V. G. Chizmeshya,*,† M. R. Bauer,‡ and J. Kouvetakis‡

Center for Solid State Science and Department of Chemistry and Biochemistry, Arizona State University, Tempe, Arizona 85287-1704

Received January 2, 2003. Revised Manuscript Received April 1, 2003

First principles density functional theory is used to study the compositional dependence of the structural, elastic, electronic, and bonding properties of newly prepared Sn_xGe_{1-x} alloys and compounds. The calculated variation of lattice constant $a(x)$ with composition for tin content (% Sn, $x < 0.20$) exhibits a small and systematic positive deviation of the lattice constants from ideal Vegard behavior, in agreement with our measurements on Sn_xGe_{1-x} alloys synthesized in this range. Over this range the compressibility also exhibits a concomitant increase relative to the Vegard average. To elucidate this structural behavior, we treat Si_xGe_{1-x}, Ge_xC_{1-x}, and Si_xC_{1-x} using the same computational procedure and find the expected negative deviations in $a(x)$ from Vegard's Law behavior in all of these cases. Calculations on molecular analogues, consisting of tetrahedral $A(XH_3)_4$ clusters with {A,X} = {Sn,Ge}, {Si,Ge}, {Si,C}, and {Ge,C}, reveal that both the sign and magnitude of the deviations from ideal behavior are also present at the molecular level. The calculated bond lengths in all of these clusters agree well with available molecular structure data for these systems.

I. Introduction

The systematic creation of epitaxial materials on Si with tunable direct band gaps is essential for future development of faster and more powerful transistors and for integration of Si-based electronics with optical components.[1−3] Our most recent discovery in this area is the synthesis of a new class of Si-based infrared semiconductors in the $Ge_{1-x}Sn_x$ system.[4,5] Novel chemical methods based on deuterium-stabilized Sn hydrides were used to prepare a broad range of highly metastable compositions and structures that cannot be obtained by conventional MBE routes.[6] Perfectly epitaxial diamond-cubic $Ge_{1-x}Sn_x$ (Sn = 2−20 at. %) alloys are created on Si(100) and exhibit high thermal stability, superior crystallinity, and unique crystallographic and optical properties such as adjustable band gaps and lattice constants. Studies of the band structure indicate band gap reductions with increasing the Sn concentration. The direct band gap (E_0) decreases from 0.72 eV for $Ge_{0.98}Sn_{0.02}$ to 0.41 eV for $Ge_{0.86}Sn_{0.14}$ compared to 0.81 eV for pure Ge. The dramatic reduction in band gap value indicates that a transition from an indirect to direct band gap is likely and thus these materials might offer a practical route to the long sought objective of developing direct-gap semiconductors on Si.

A systematic study of the crystal structure by high-resolution electron microscopy, and electron and X-ray diffraction, indicate that the films grow essentially strain-free and display lattice constants that are intermediate to those of Ge (5.658 Å) and α-Sn (6.493 Å). Here, we report the lattice constants for a number of well-crystallized SnGe alloys (% Sn < 20%) for the first time. A striking feature of the data is that they exhibit a systematic positive departure from Vegard's rule. This is in direct contrast with the compositional variation of the lattice constant in the classic $Si_{1-x}Ge_x$, $Si_{1-x}C_x$, and $Ge_{1-x}C_x$ group IV alloys which exhibit negative bowing of the lattice constant relative to linear behavior.

Examples in which the linear rule is strictly obeyed are very rare in binary alloys, and since the appearance of Vegard's work in 1921, a large number of papers have been written concerning *deviations* from Vegard's Law. The first comprehensive review of these theories was provided by Gschneidner and Vineyard,[7] who compared observed deviations from Vegard's Law for 44 binary alloy systems with theoretical models proposed by Pines,[8] Jaswon et al.,[9] Fournet,[10] Zen,[11] and Sarkisov.[12] With the exception of the Sarkisov approach, which is

* Corresponding author. E-mail: chizmesh@asu.edu.
† Center for Solid State Science.
‡ Department of Chemistry and Biochemistry.

(1) Wang, P.; Krespi, V.; Chang, E.; Louie, S. G.; Cohen, M. L. *Nature* **2001**, *409*, 69.
(2) Wang, P.; Krespi, V.; Chang, E.; Louie, S. G.; Cohen, M. L. *Phys Rev. B* **2001**, *64*, 23 5201.
(3) He, G.; Atwater, H. A. *Phys. Rev. Lett*. **1997**, *79*, 19973.
(4) Bauer, M.; Taraci, J.; Tolle, J.; Chizmeshya, A. V. G.; Zollner, S.; Menendez, J.; Smith, D. J.; Kouvetakis, J. *Appl. Phys. Lett.* **2002**, *81*, 2992.
(5) Taraci, J.; Mc Cartney, M. R., Menendez, J.; Zollner, S.; Smith, D. J.; Haaland, A.; Kouvetakis, J. *J. of the Am. Chem. Soc.* **2001**, *123*, 10980.
(6) Gurdal, O.; Desjardins, R.; Carlsson, J. R. A.; Taylor, N.; Radamson, H. H.; Sundgren, J.-E.; Greene, J. E. *J. Appl. Phys.* **1998**, *83*, 162.
(7) Gschneidner, K.A; Vineyard, G. H. *J. Appl. Phys.* **1962**, *33*, 3444.
(8) Pines, B. J. *J. Phys.* **1940**, *3*, 309.
(9) Jawson, M. A.; Henry, W. G.; Raynor, G. V. *Proc. Phys. Soc.* **1951**, *64*, 177.
(10) Fournet, G. J. *Phys. Radium* **1953**, *14*, 374.
(11) Zen, E-an *Am. Miner.* **1956**, *41*, 523.
(12) Sarkisov, E. S. *Zh. Fiz. Khim*. **1960**, *34*, 432.

10.1021/cm0300011 CCC: $25.00
Published on Web 06/24/2003

based on a free electron-gas concept, all of the latter models invoke a first-order elastic strain expansion of the alloy energy to explain the magnitude and sign of the deviations from Vegard's Law. Unfortunately, none are able to correctly predict the sign and/or magnitude of the observed deviations, even when second-order elasticity theory is employed.[7] Among these, Fournet's theory is arguably the simplest, involving only the isotropic compressibilities and lattice constants of an alloy's constituent end members. Other notable recent attempts at a systematic explanation of deviations from Vegard's Law include the work of Hafner who, like Sarkisov, invokes the free-electron gas model to estimate the elastic effects on the formation volume of simple-metal binary alloys.[13] As we will show below, the observed behavior in SnGe alloys cannot be explained using either Fournet's theory,[10] or the recent electron gas theory of Hafner,[13] although the latter method does provide a qualitative account of the magnitude of the deviations in relation to related systems such as Si_xC_{1-x}, Ge_xC_{1-x}, and Si_xGe_{1-x}. The inability of these theories to account for the observed behavior prompted us to undertake an ab initio study of the problem. Our main objective here is to elucidate the composition−structure relationship in SnGe alloys in the range of Sn compositions $x < 20\%$, for which direct comparisons with newly synthesized alloys can be performed, using first principles simulation.

Ab initio density functional theory methods have already been applied to the study of a wide range of Sn_xGe_{1-x} materials in which $x > 25$ at. %. For example, the stability, band structure, and optical properties of the $Sn_{0.5}Ge_{0.5}$ phase were recently investigated using a total-energy LCAO-DFT method[14] within the generalized gradient approximation (GGA). Using empirical corrections to the computed GGA band energies, a small direct gap of 0.1 eV was predicted for SnGe, while a positive deviation of 0.005 Å from Vegard's average is reported for the alloy. In another recent work Shen et al. presented a theoretical analysis of random alloys for a number of discrete Sn compositions (0, 25%, 50%, 75%, and 100%). Using statistical averaging over several random configurations at each composition, they find that random alloys are slightly less metastable than their ordered counterparts in the zinc blende structure. These authors also report a slight positive departure from expected Vegard behavior for the lattice constants of the intermediate compositions, although this finding is not emphasized in the work. Nevertheless, the above systems have not yet been synthesized.

The following section briefly describes the experimental procedures used to obtain the structural data for the newly prepared Sn_xGe_{1-x} with $x = 0.02-0.20$. We then outline the calculation of the structural and elastic properties of each alloy in the % Sn < 20 composition range. These ab initio predictions are compared with the simplified treatment of alloy behavior due to Fournet, and the electron gas model of Hafner. To further elucidate the structural behavior of these extended solid phases, we then conduct an analysis from the point of view of molecular analogues. We show that the sign and magnitude of the deviations from ideal behavior in the alloys are already present at the molecular level in tetrahedral $A(XH_3)_4$ clusters with {A,X} = {Sn,Ge}, {Si,Ge}, {Si,C}, and {Ge,C}.

II. Experimental Section

The synthesis of $Ge_{1-x}Sn_x$ alloys is achieved using a novel chemical vapor deposition (CVD) synthesis approach based on deuterium-stabilized Sn hydrides precursors, which provide a new low-temperature route to a broad range of highly metastable compositions and structures that cannot be obtained by other methods.

$$SnD_4 + Ge_2H_6 \rightarrow Ge_{1-x}Sn_x/H_2(g) \quad (1)$$

Perfectly epitaxial and completely monocrystalline diamond-cubic $Ge_{1-x}Sn_x$ film heterostructures were grown on Si(100) between 275 and 350 °C. Because the films are largely strain-free and of such high quality, individual optical transitions can be easily identified and compared with those in pure Ge. Recently, we carried out a series of spectroscopic ellipsometry measurements (UV−visible and IR) to characterize the E_1, $E_1 + \Delta_1$, E_0*, and E_0 electronic transitions in $Ge_{1-x}Sn_x$. These measurements suggest that the band structure of the alloys is qualitatively very similar to that of pure Si, Ge, and α-Sn. This allows a straightforward interpretation of the critical point dependence on concentration. Our data show that the values of the E_1 and $E_1 + \Delta_1$, and E_0* critical points decrease systematically with increasing Sn concentration. In particular, the direct band gap, E_0, decreases dramatically from 0.81 eV in pure Ge to 0.41 eV in $Sn_{0.14}Ge_{0.86}$.[15] Additional details are provided elsewhere.[16,17]

To determine the quality of epitaxial growth and evaluate the Sn substitutionality in the Ge lattice, RBS random and aligned spectra were recorded and compared. Parts (a) and (b) of Figure 1 show spectra for samples containing 2 and 14% Sn, respectively. It is evident that both Sn and Ge channel remarkably well despite the large difference in lattice constants between the film and the substrate. These remarkable channeling results provide unequivocal proof that Sn *must* occupy substitutional tetrahedral sites in the diamond-cubic structure in our CVD-grown films. The degree of substitutionality between Ge and Sn in the same sample can be determined from χ_{min}, which is the ratio of the aligned vs random peak heights. For both Ge and Sn in the $Ge_{0.98}Sn_{0.02}$ sample we obtain a value of $\chi_{min} \sim 4\%$, while $\chi_{min} \sim 50\%$ in the $Ge_{0.86}Sn_{0.14}$ sample, indicating that all of the Sn is substitutional. The 4% value approaches the practical limit of about 3% for structurally perfect Si, which is unprecedented for a binary crystal grown directly on Si. The large χ_{min} value found in $Ge_{0.86}Sn_{0.14}$ is likely due to some mosaic spread in the higher Sn-content crystal due to the increase in lattice mismatch. Overall, the channeling data indicate that the Ge−Sn samples are monocrystalline and epitaxial.

The structural properties of these films were also studied by high-resolution cross-sectional electron microscopy (XTEM) and high-resolution X-ray diffraction. The XTEM studies revealed thick single-crystal layers with remarkably low concentrations of threading defects. An electron micrograph demonstrating nearly defect-free heteroepitaxial growth of $Ge_{0.94}Sn_{0.06}$ is also shown in Figure 1c. High-resolution X-ray measurements in the $\theta-2\theta$ mode showed a single, strong peak corresponding to the (004) reflection of the diamond-cubic lattice. In-plane rocking scans of the (004) reflection have a full-width-at-half-maximum between 0.25 and 0.50, indicating

(13) Hafner, J. *J. Phys. F: Met. Phys.* **1985**, *15*, L43.
(14) Pandey, R.; Rerat, M.; Causa, M. *Appl. Phys. Lett.* **1999**, *75*, 4127.
(15) Bauer, M. et al. (submitted to *Nature*).
(16) Taraci, J.; Tolle, J.; Kouvetakis, J.; McCartney, M. R.; Smith, D. J.; Menendez, J.; Santana, M. A. *Appl. Phys. Lett.* **2001**, *78*, 3607.
(17) Taraci, J.; Zollner, S.; McCartney, M. R.; Menendez, J.; Santana-Aranda, M. A.; Smith, D. J.; Haaland, A.; Tutukin, A. V.; Gundersen, G.; Wolf, G. H.; Kouvetakis, J. *J. Am. Chem. Soc.* **2001**, *123*, 10980.

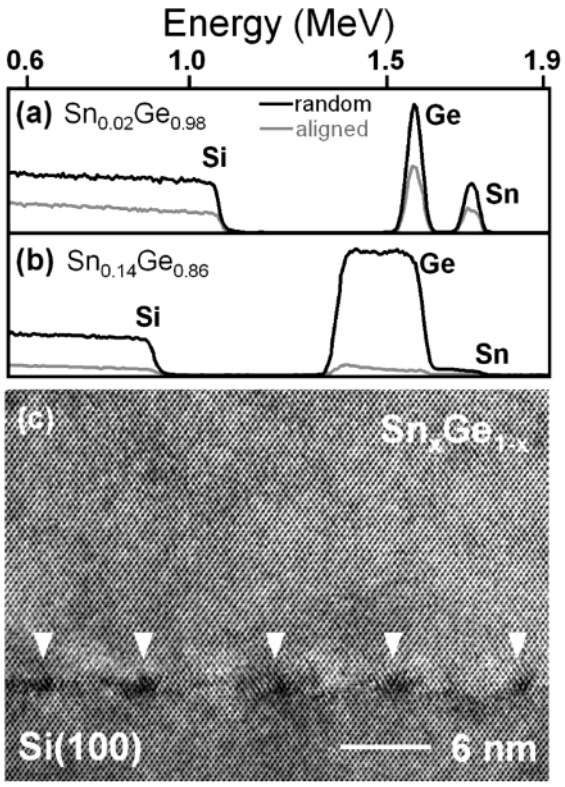

Figure 1. (a) RBS aligned (gray trace) and random spectra of $Ge_{0.98}Sn_{0.02}$ with near perfect crystallinity. Channeling of Sn and Ge approaches the theoretical limit of pure Si. (b) Aligned and random spectra for $Ge_{0.86}Sn_{0.14}$ show the same χ_{min} for both Ge and Sn, indicating that the entire Sn content is substitutional. (c) High-resolution electron micrograph of the interface region in $Ge_{0.94}Sn_{0.06}$ showing virtually perfect epitaxial growth. Arrows indicate the location of misfit dislocations.

a tightly aligned spread of the crystal mosaics. Similar widths of rocking curves are found for other relaxed heteroepitaxial films with a large lattice mismatch relative to the substrate. The unit cell parameters obtained from the (004) reflection for samples containing 2, 3, 4, 8, 11, 15, 18, and 19 at. % Sn (as measured by RBS) were 5.672, 5.694, 5.711, 5.748, 5.761, 5.802, 5.831, and 5.833 Å, respectively, where the average standard deviations range from ±0.001 to ±0.003 Å. These values are intermediate to those of Ge (5.657 Å) and α-Sn (6.489 Å) and increase monotonically with increasing Sn concentration. Virtually identical values were obtained for each sample from measurements of the selected area electron diffraction patterns (SAED).

Digital diffractogram analysis of selected XTEM images closely confirmed the measured values of the unit cell edges and also showed that the lattice parameter did not vary locally throughout the sample. The experimental unit cell parameters, *a*, the corresponding Sn−Ge concentration estimated from Vegard's Law (which assumes linear interpolation between the unit cell parameters of Ge and α-Sn), and the concentration of Sn as measured by RBS are listed in Table 1. Also included in this table are the results of our theoretical calculations (described below) for the lattice constants as a function of Sn for ordered alloys. Figure 2 is a graphical representation of these trends. A striking feature of the data is that a positive deviation from Vegard's Law is found for both the experimental and theoretical values of the lattice constants (see Figure 2). This is in direct contrast with the compositional variation of the lattice constants in the classic $Si_{1-x}Ge_x$ and $Si_{1-x}C_x$ group IV alloys. In these systems the deviations from Vegard's Law are negative, as illustrated by numerous experimental and theoretical studies.

Table 1. Observed and Calculated Lattice Parameters of $Ge_{1-x}Sn_x$[a]

observed			calculated			
% Sn	*a*(Vegard)	*a*(observed)	% Sn	Sn/Ge	*a*(Vegard)	*a*(calculated)
0	5.658	5.658	0	0	5.626	5.626
2	5.675	5.672	1.6	1/64	5.639	5.639
3	5.683	5.694	3.1	2/64	5.652	5.653
4	5.691	5.711	6.3	4/64	5.678	5.683
8	5.725	5.748	12.5	8/64	5.729	5.737
11	5.750	5.761	18.8	12/64	5.781	5.792
15	5.783	5.802	100	1	6.456	6.456
18	5.808	5.831				
19	5.817	5.833				

[a] The observed lattice parameter composition dependence in the range 0−18% Sn content is compared with Vegard's Law. The calculated values are obtained from a first principles LDA static lattice calculation. All values are reports in Angstroms. The standard deviations on all experimental values are within ±0.003.

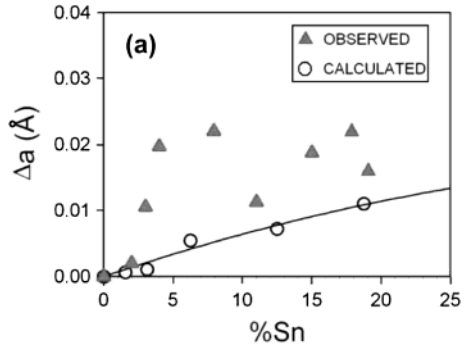

Figure 2. Observed and calculated deviations of the lattice parameters of $Ge_{1-x}Sn_x$ from Vegard's Law. The observed lattice constant deviations in the range 0−18% Sn content (solid triangles) are compared with first principles LDA static lattice calculation (hollow circles). All values are reported in Angstroms. The absolute standard deviations on the XRD-derived lattice constant values is less than ±0.003 Å over the entire composition range (not shown in figure).

III. First Principles Calculations

The unexpected synthetic and structural properties described above prompted us to undertake a series of ab initio calculations aimed at elucidating the electronic, energetic, and structural properties of $Ge_{1-x}Sn_x$ materials. The first principles density functional theory results were obtained using the Vienna ab initio simulation package (VASP), which uses transferable ultra-soft pseudopotentials to efficiently treat ion−electron interactions, and the Ceperley-Alder exchange-correlation implementation of the local density approximation (LDA).[18,19] Electronic states were expanded in a plane-wave basis and the convergence of electronic properties was achieved with a kinetic energy cutoff of 600 eV and using a Monkhorst-Pack grid consisting of 10 irreducible *k*-points for the Brillouin zone integrations.

The discrete tin concentrations (0−20% range) found in the actual samples were modeled by adopting a 64-atom supercell constructed from a 2 × 2 × 2 repeat of the basic 8-atom diamond lattice unit cell. While it is well-known that Sn undergoes a cubic-tetragonal structural transition, our microstructural analysis indicates perfectly diamondlike material. All of our simulations

(18) Kresse, G.; Furthmuller, J. *Comput. Mater. Sci.* **1996**, *6*, 15. Kresse, G.; Hafner, J. *Phys. Rev. B* **1993**, *47*, 558. Kresse, G.; Furthmuller, J. J. *Phys. Rev. B* **1996** *54*, 11.
(19) Ceperley, D. M.; Alder, B. J. *Phys. Rev. Lett.* **1980**, *45*, 566.

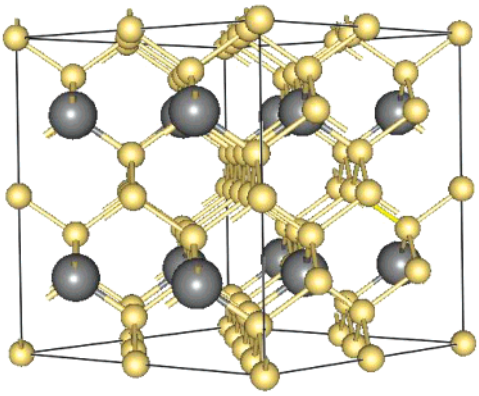

Figure 3. Supercell representation of the $Sn_{0.12}Ge_{0.88}$ ordered structure model representing an alloy with a tin-to-germanium ratio of 8/64. Germanium atoms, gold; tin atoms, dark gray.

are therefore based on a diamond lattice template with Sn and Ge distributed on the various sites to form an alloy structure. The initial lattice configuration for each alloy was obtained by distributing tin atoms in a highly symmetrical fashion which maximizes Sn−Sn nearest neighbor distances and minimizes the number of heteropolar bonds within the supercell. For example, an ordered lattice with a Sn/Ge ratio of 4/64 has a tetrahedral arrangement of tin atoms occupying the 4d sites in the $Fd\bar{3}m$ space group. A body-centered arrangement with space group $I\bar{4}3m$ and tin on the 2a sites is used for the 2/64 tin concentration. The $P\bar{4}3m$ space group can accommodate configurations with Sn/Ge ratios of 1/64 (tin on the 1a site) and 8/64 (tin on 1a, 1b, 3c, and 3d sites). Finally, the 12/64 (∼19% tin) possesses the lowest symmetry, with tin atoms occupying all the doubly degenerate symmetry sites (2a, ..., 2f) within the $P\bar{4}2c$ space group. An example of an ordered structure model is shown in Figure 3, which represents an alloy with a tin-to-germanium ratio of 8/64 (e.g., $Sn_{0.12}Ge_{0.88}$).

For each alloy considered, an energy−volume data set was computed by varying the system volume over a range spanning −10% to 40% around equilibrium. No shape constraints were imposed upon the supercell and all ionic forces were minimized to an accuracy of <0.001 eV/Å, yielding fully relaxed ionic positions at each fixed supercell volume. The resulting energy−volume data were then fitted to a third-order Birch−Murnaghan equation of state[20] to obtain the cohesive energy, equilibrium lattice constant, bulk modulus, and bulk modulus pressure derivative at ambient pressure. These results are listed in Table 2. All state properties were computed in the static lattice limit and therefore neglect free energy contributions due to lattice vibrations (e.g., thermal expansion). In this approximation our calculated equilibrium lattice constants and bulk moduli are 5.626 Å and 71 GPa for germanium,[21] and 6.456 Å and 45 GPa for α-Sn,[22] respectively. These compare very well with their experimental counterparts $a_{Ge} = 5.658$ Å, $B_{Ge} = 77$ GPa and $a_{\alpha-Sn} = 6.493$ Å, $B_{\alpha-Sn} = 43$ GPa. The formation energy at fixed tin concentration, calculated as the cohesive energy difference between the alloy and that of a stoichiometric equivalent sum of elemental

(20) Birch, F. *J. Geophys. Res.* **1987**, *83*, 1257.
(21) Cohen, M. L.; Chelikowsky, J. R. *Electronic Structure and Optical Properties of Semiconductors*; Springer: New York, 1988.
(22) Ravelo, R.; Baskes, M. *Phys. Rev. Lett.* **1997**, *79*, 2482.

Table 2. Compression Equation of State Parameters Obtained by Fitting the First Principles Energy Volume Data to a Third-Order Birch−Murnaghan Equation of State[a]

Sn	Ge	% Sn	E_0 (Hartree)	a_0 (Å)	V_0 (Å^3)	B_0 (GPa)	B_0'
0	64	0.00	−12.22546	11.251	1424.3	70.81	4.76
1	63	1.56	−12.19121	11.279	1434.7	70.16	4.76
2	62	3.13	−12.15829	11.305	1445.0	69.47	4.75
4	60	6.25	−12.07905	11.366	1468.3	67.97	4.71
8	56	12.50	−11.95013	11.473	1510.3	65.79	4.71
12	52	18.75	−11.84142	11.584	1554.5	63.92	4.66
64	0	100.00	−10.58741	12.912	2152.7	44.62	4.65

[a] The total energy parameter, E_0, is the cohesive energy per unit cell (64 atoms) relative to an equivalent stoichiometric number of free neutral atoms. Energy values are reported in Hartree units (1 Hartree = 27.2116 eV), lengths in Angstroms, and moduli in GPa.

tin and germanium, is found to be positive for all alloys, indicating that the solid solutions are slightly metastable by a few kJ/mol (e.g., ∼0.4, 0.7, 1.8, 2.9, and 3.7 kJ/mol per atom corresponding to 1.56, 3.13, 6.25, 12.5, and 18.75% Sn, respectively). These alloys are therefore expected to be thermodynamically accessible under the experimental conditions described above.

The composition dependence of elastic moduli in bulk stoichiometric $Ge_{1-x}Sn_x$ ordered alloys is also of interest from the point of view of film growth and stability. When the fixed volume internal structure optimizations described above were carried out, no shape constraint was imposed upon the computational cells. The associated stress tensor exhibited negligible anisotropy, indicating no departure from cubic symmetry. After each complete equation of state determination (at each composition), we also performed a highly accurate full stress relaxation starting with a volume and lattice configuration close to equilibrium and obtained the same equilibrium volume as determined from an energy−volume fit. On the basis of these calculations, thermodynamically metastable $Ge_{1-x}Sn_x$ films are expected to be mechanically stable, although a definitive conclusion should be based on an examination of Born stability criteria and their dependence on concentration. Our calculations also indicate that an increase in the compressibility of the alloys is expected, above and beyond the expectation based on a Vegard estimate. This is concomitant with the slight (0.1−0.2%) positive deviation of the lattice constant from Vegard's Law. However, the fractional increase in the compressibility is much larger. This is illustrated in Figure 4, which shows a corresponding depression of the alloy bulk moduli from Vegard's Law, approaching $\Delta B_0/B_0 \sim 3\%$ for 18.75% Sn.

IV. Deviations from Vegard's Law: A Molecular Perspective

A striking feature of the results presented in Table 1 and Figure 2 is that a systematic positive deviation from Vegard's Law is found for both the experimental and theoretical lattice constants. The opposite behavior is observed in the related $Si_{1-x}Ge_x$ and $Si_{1-x}C_x$ group IV binary alloys. However, positive lattice constant deviations of comparable magnitude to those found here have been reported for other pseudo-binary and ternary systems, such as $Al_xGa_{1-x}/GaSb$[23] and $Al_xGa_{1-x}As$.[24] It has even been suggested that lattice constant deviations from Vegard's Law are present in all semiconductors

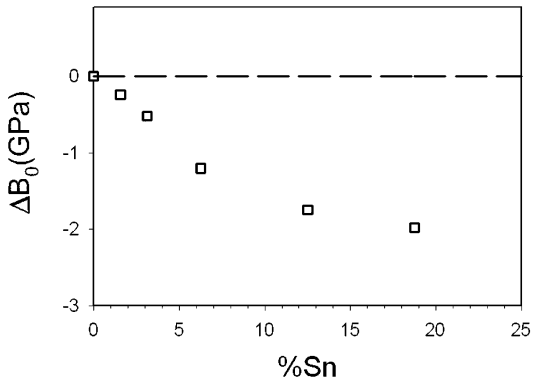

Figure 4. Calculated deviations of the bulk moduli of $Ge_{1-x}Sn_x$ alloys from Vegard's Law (hollow squares). The dashed line represents the Vegard average. All values are reported in GPa.

and have positive signs for zinc blende ternary alloys and negative signs in diamondlike alloys.[25] Such deviations from ideal behavior are often qualitatively discussed in terms of ionic size ratios, elastic behavior, and electronegativity differences but a detailed quantitative understanding of their origin is, unfortunately, still lacking, particularly in the case of the ubiquitous binary compounds. In view of the important role of binary group IV alloys in modern semiconductor technology, and the need to expand our understanding of these systems, a systematic explanation for the magnitude and polarity of the deviation in terms of the intrinsic properties of the constituent elements is highly desirable.

To investigate the origin of the positive lattice constant deviations found in Ge_xSn_{1-x} ($x < 20\%$), two conceptually distinct, but complementary, strategies were pursued. The first compares the Ge_xSn_{1-x} system directly with the well-known Si_xGe_{1-x} and Si_xC_{1-x} systems in which deviations of the lattice constant from Vegard's Law are known to be negative. In addition, there are abundant bonding data available for Si−Ge and Si−C solids, films, and molecules that allowed for the prediction of the bonding properties of these systems. We will demonstrate that the same computational conditions and procedures used to predict the negative deviations in Si_xGe_{1-x} and Si_xC_{1-x} also yield positive deviations in the Ge_xSn_{1-x} system. This not only provides support for our conclusions regarding the Sn−Ge system but also yields new insight into the origin of the opposite behavior in Si−Ge and Si−C.

The second strategy is to calculate the bonding trends in the Sn−Ge, Si−Ge, and Si−C systems using molecular model compounds containing tetrahedral cores such as $SnGe_4$, Ge_4Sn, $SiGe_4$, Ge_4Si, and CSi_4. This approach is based on the well-established, systematic correspondence between the bond lengths in such molecules and their extended solid counterparts. For example, the Si−C bond length in silicon carbide is nearly identical to that found in most molecular systems containing Si_4C tetrahedral cores [i.e., $C(SiH_3)_4$]. This is also borne out by our explicit ab initio calculations, as we shall demonstrate below (Table 3). To simplify our analysis of bonding trends in molecular systems and solids, we restrict our attention to 50% alloys such as $Si_{0.50}Ge_{0.50}$, $Si_{0.50}C_{0.50}$, and $Sn_{0.50}Ge_{0.50}$ and to the corresponding tetrahedral clusters such as $Si(GeR_3)_4$, $Ge(SiR_3)_4$, $C(SiR_3)_4$, $Sn(GeR_3)_4$, $Si(CR_3)_4$, and $Ge(SnR_3)_4$ (R = Me,H), which share the same tetrahedral building blocks with the 50% alloys. For these 50/50 compositions deviations from Vegard's Law are also expected to be maximal.

The systematic comparison of bonding trends in isolated clusters and corresponding extended solid-state structures can be achieved by introducing two bond length averages: $b_{iso} = (b_{AA} + b_{XX})/2$ and $b_{aniso} = (b_{AX} + b_{XA})/2$. The quantity b_{iso} is simply the average value of the homonuclear bonds in the system. It coincides *exactly* with the Vegard average of a 50% alloy composed of A and X. Note that this definition holds for both clusters and solids. In analogy, b_{aniso} is the average of the heteronuclear bond lengths formed in mixed clusters or the corresponding extended solids. In the context of clusters, this is a measure of the average A−X bond length while in the extended solid it simply related to the lattice constant for the alloy. For example, in diamond-cubic-based systems b_{aniso} is the bond length deduced directly from the lattice constant, a, via the relation $b_{aniso} = a\sqrt{3}/4$. *In the special case of a 50% alloy, the difference between* b_{aniso} *and* b_{iso} *represents the deviation from ideal Vegard behavior*. Our approach here is to calculate b_{iso} and b_{aniso} for both AX alloys and the corresponding $A(XH_3)_4$ tetrahedral molecular clusters (see Figure 5), where {A,X} = {C,Si,Ge,Sn} to determine whether the positive/negative deviations obtained in the alloys are also present at the more fundamental molecular level.

We begin by computing the ground-state structures of elemental diamond-cubic C, Si, Ge, and Sn and that of the 50% alloys $Si_{0.50}C_{0.50}$, $Si_{0.50}Ge_{0.50}$, and $Sn_{0.50}Ge_{0.50}$.[26] For elemental Ge and Sn the values obtained are identical to those reported in the previous section (see also Table 1), while for Si the lattice constant and bulk modulus are calculated to be $a_{Si} = 5.3894$ Å and $B_{Si} = 96$ GPa, respectively. These are in good agreement with the corresponding experimental values $a_{Si} = 5.432$ Å and $B_{Si} = 101$ GPa. We find similar good agreement for elemental C (diamond) for which $a_C = 3.527$ Å and $B_C = 465$ GPa compared with the experimental values 3.570 Å and 441 GPa for the lattice constant and bulk modulus, respectively. The 50% alloy properties were computed using the same procedure.

The corresponding lattice constants and bulk moduli of the $Si_{0.50}Ge_{0.50}$ and $Sn_{0.50}Ge_{0.50}$ alloys are predicted to be $a_{SnGe} = 6.0510$ Å, $B_{SnGe} = 55.6$ GPa, $a_{SiGe} = 5.4993$ Å, and $B_{SiGe} = 84$ GPa while for $Si_{0.50}C_{0.50}$ we find a_{SiC}

(23) Wasilewski, Z. R.; Dion, M. M.; Lockwood, D. J.; Poole, P.; Streater, R. W.; Springthorpe, A. J. *J. Appl. Phys.* **1997**, *81*, 1683.

(24) Bocchi, X.; Franchi, S.; Germini, F.; Baraldi, A.; Magnanini, R.; De Salvador, D.; Berti, M.; Drigo, A. V. *J. Appl. Phys.* **1999**, *86*, 1298.

(25) De Salvador, D.; Berti, M.; Bocchi, C.; Sambo, A.; Drigo, A. V.; Baraldi, A.; Magnanini, R.; Franchi, S.; Germini, F. Laboratori Nazionali de Lignaro Annual Report 2000, p 116.

(26) The high symmetry of the 50% alloys permits a small 8-atom diamond lattice unit cell to be used for the extended solid-state calculations. The concomitant reduction in computational effort allows a higher degree of computational precision to be attained: an energy cutoff of 600 eV is used to expand the electronic properties while 60 irreducible *k*-points are used to perform the reciprocal space integrations. The equations of state are obtained using the same procedure as described for the 64-atom cell calculations and here we find the same values for the bulk moduli and lattice constants in the case of α-Sn and Ge.

Table 3. Comparison of Bond Lengths in the Sn−Ge, Si−Ge, Si−C, and Ge−C Systems within the Molecular (Cluster) and Solid-State Settings[a]

	Sn−Ge					Si−Ge			
	cluster		solid			cluster		solid	
bond	theory	expt.	theory	expt.	bond	theory	expt.	theory	expt.
b_{SnSn}	2.740		2.796	**2.812**	b_{SiSi}	2.310	**2.356**[28]	2.334	**2.3517**
b_{GeGe}	2.386		2.436	**2.450**	b_{GeGe}	2.386	**2.435**[27]	2.436	**2.4500**
b_{iso}	2.563		2.6157	2.631	b_{iso}	2.348	2.396	2.3848	2.4009
b_{SnGe}	2.567				b_{SiGe}	2.3460	**2.383**[26]		
b_{GeSn}	2.568	**2.593**[29]			b_{GeSi}	2.3465	**2.396**[26]		
b_{aniso}	2.5675		2.6202		b_{aniso}	2.3463	2.390	2.3813	**2.3979**[26]
δb	0.0045		0.0045		δb	−0.0018	**−0.0055**	−0.0035	**−0.0030**

	Si−C					Ge−C			
	cluster		solid			cluster		solid	
bond	theory	expt.	theory	expt.	bond	theory	expt.	theory	expt.
b_{SiSi}	2.3103	**2.356**[28]	2.3337	**2.3517**	b_{GeGe}	2.386	**2.435**[27]	2.436	**2.4500**
b_{CC}	1.5125	**1.539**[37]	1.5273	**1.5459**	b_{CC}	1.5125	**1.539**[37]	1.5273	**1.5459**
b_{iso}	1.9114	1.9475	1.9305	1.9488	b_{iso}	1.9493	1.987	1.9817	1.9980
b_{SiC}	1.8598	**1.877**[38]			b_{GeC}	1.9349	**1.945**[35]		
b_{CSi}	1.8520	**1.875**[36]			b_{CGe}	1.9381	**1.970**[34]		
b_{aniso}	1.8559	1.876	1.8705	**1.8875**[26]	b_{aniso}	1.9365	1.9575	1.9615	
δb	−0.0555	**−0.0720**	−0.0600	**−0.0613**	δb	−0.0128	**−0.0295**	−0.0202	

[a] The theoretical values for all molecular and solid-state systems were obtained using the same computational procedures as described in the text. The average of homonuclear and heternuclear bond lengths within a binary system are denoted by b_{iso} and b_{aniso}, respectively. For a solid b_{iso} is equivalent to the Vegard average while b_{aniso} corresponds to the average bond length at a composition of $x = 0.50$. Experimental values are in bold face font. All values given in Angstroms.

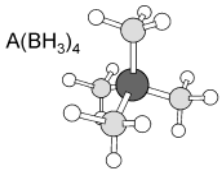

Figure 5. Schematic representation of the molecular structure of $A(XH_3)_4$ used in the ab initio calculations of cluster properties.

= 4.3197 Å, B_{SiC} = 225 GPa. Using these results, and our calculated lattice constants for C, Si, Ge, and Sn, we can immediately obtain deviations from Vegard's Law for the 50% alloys. For $Sn_{0.50}Ge_{0.50}$ we obtain $a_{SnGe} - (a_{Sn} + a_{Ge})/2 = +0.01$ Å and for $Si_{0.50}Ge_{0.50}$ our calculations yield $a_{SiGe} - (a_{Si} + a_{Ge})/2 = -0.008$ Å while for the carbide $a_{SiC} - (a_{Si} + a_C)/2 = -0.128$ Å. The positive deviation found in the SnGe alloy is consistent with the trend found in our supercell calculations and our experimental observations for Ge_xSn_{1-x}, $x < 20\%$ (i.e., positive deviation from Vegard's Law), while the predicted negative deviations found for SiGe and SiC are in excellent agreement with experiment (see Table 3).

The calculation of the bonding properties for the $A(XH_3)_4$ molecular clusters is also straightforward and was carried out using the VASP code[18] using the same computational procedures and approximations as for the solids above.[27] The main results are presented in Table 3, which lists the equilibrium bond lengths for both the extended solid and molecular Sn−Ge, Si−Ge, and Si−C systems. For all molecular systems the anisotropic bond lengths are nearly independent of ordering, namely, $|b_{AX} - b_{XA}| < 0.004$ Å in carbide clusters, whereas $|b_{AX} - b_{XA}| < 0.0005$ Å in the heavier Sn and Ge bearing clusters. The average heteronuclear bond lengths, b_{aniso}, are 1.8559, 2.3468, and 2.5675 Å for Si−C, Si−Ge, and Sn−Ge, respectively. As discussed earlier, the corresponding isotropic average bond lengths, b_{iso}, are analogous to an exact Vegard average in the solid system. In the molecular setting we obtain 2.5630 Å for the Sn−Ge and 2.3480 Å for Si−Ge. The deviations from isotropic bonding in molecules is thus $\delta b = b_{aniso} - b_{iso} = +0.0045$ Å for Sn−Ge and $\delta b = -0.0018$ Å for the Si−Ge. Remarkably, these values are very close to those in the extended solid calculations where $\delta b = +0.0045$ Å for $Sn_{0.50}Ge_{0.50}$, and $\delta b = -0.0035$ Å for $Si_{0.50}Ge_{0.50}$. Significantly larger departures from ideal behavior are found in the silicon carbide system where $\delta b = -0.0555$ Å for Si−C-based molecules while a similar value of $\delta b = -0.0600$ Å is found in the solid phase $Si_{0.50}C_{0.50}$ alloy. Thus, the sign and magnitude of δb is, to first approximation, the same in molecules and solids for Si−C, Si−Ge, and Sn−Ge. For the class of tetrahedrally coordinated compounds analyzed here it appears that the subtle effects of second neighbor interactions are not required to account for the key deviations in bonding anisotropy. A survey of the trends in bond lengths between clusters and solids (moving across rows in Table 3) clearly reveals that bond lengths in solids are systematically ∼1−2% larger than those in the corresponding molecule.

To further support these findings, we have extended the foregoing analysis to the less studied GeC system for which molecular structure data do exist. The solid-phase alloys have not yet been synthesized, yet our analysis demonstrates that for molecular clusters the trends are like those in the SiC system. In particular, for Ge−C clusters we obtain $\delta b = -0.0128$ Å, which compares well with the experimentally derived values

(27) The calculation of molecular properties is therefore also carried out using the VASP code.[15] A 600-eV cutoff energy was used in the expansion of electronic properties, while a single *k*-point was found to be sufficient for the Brillouin zone sampling. The minimum energy molecular structures were all obtained by placing clusters within a periodic cubic supercell with an edge length of 20 Å and then relaxing all atomic positions. Highly accurate ground-state structures were obtained by converging the residual forces to a value <0.001 eV/Å.

of $\delta b = -0.0295$ Å. A very similar value of $\delta b = -0.0202$ Å is found for the solid-phase deviation. These results indicate that Ge−C displays negative deviations from Vegard's Law compared to what we found for Si−C and Si−Ge.

V. Discussion

The negative deviations calculated for the Si−C and Si−Ge cluster molecules and alloys can in fact be corroborated by experimental data and this is also shown in Table 3. For the clusters, the values for the Si−Si, Si−Ge, and Ge−Si bond lengths are obtained from the crystal structures of the compounds $Si(SiMe_3)_4$ (and hydride derivatives), $Si(GeMe_3)_4$, and $Ge(SiMe_3)_4$, respectively.[28−30] The Ge−Ge bond length value of 2.435 Å was estimated from mixed clusters incorporating the $Ge(SiGe)_2$ core since $Ge(GeR_3)_4$ (R = Me, H etc.) has not yet been synthesized. From these experimental data b_{iso} is found to be 2.396 Å, while b_{aniso} has the value 2.390 Å. The experimentally derived devation is therefore $\delta b = -0.0055$ Å, which is of the same sign, but somewhat larger in magnitude, than the predicted value $\delta b = -0.0012$ Å. The slight discrepancy between the calculated and observed values may be due to the neglect of thermal motion, for example, zero point energy and vibrational free energy, in the model clusters which possess additional (e.g., librational) degrees of freedom. In addition, the experimental values were obtained from a variety of molecules containing different terminal groups including methyl, hydrogen, and $SiMe_3$. All of these effects can contribute to slight variations in the {Si,Ge} bond lengths. For the extended $Si_{0.50}Ge_{0.50}$ solid the lattice constant deviation from Vegard's Law is well-known to be negative ($\delta b = -0.0031$ Å, see Table 2). This value is very well reproduced by the present study, which finds $\delta b = -0.0035$ Å.

For the SnGe system, an extensive comparison including both solid-state and molecular systems is not possible due to the lack of experimental data. Nevertheless, we were able to obtain the average Ge−Sn bond lengths from the crystal structure of tetrakis(trimethylstannyl)germane, $(Me_3Sn)_4Ge$, which we recently synthesized.[31−33] The structural ORTEP model of $Ge(SnMe_3)_4$ is shown in Figure 6, while the associated

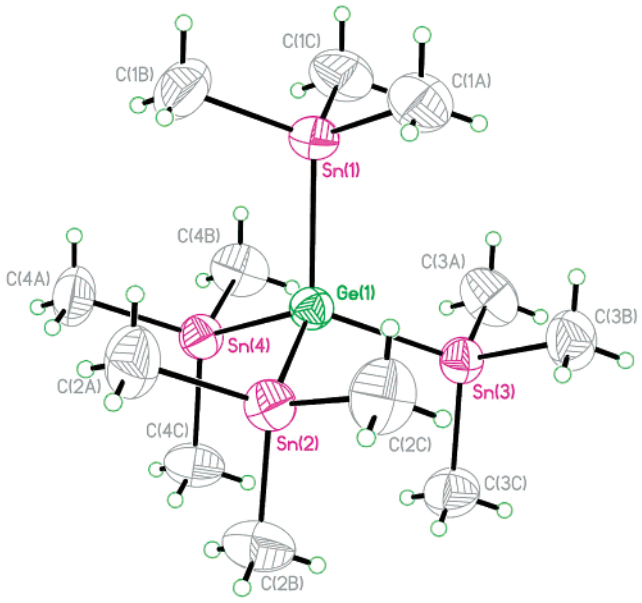

Figure 6. ORTEP diagram corresponding to the X-ray structural determination of the condensed molecular form of $Ge(SnMe_3)_4$.

Table 4. Bond Distances and Bond Angles Associated with the ORTEP Structure Shown in Figure 5[a]

bond distance (Å)		bond angle (deg)	
Ge(1)Sn(1)	2.5952	Sn(1)Ge(1)Sn(2)	110.83
Ge(1)Sn(2)	2.5953	Sn(1)Ge(1)Sn(3)	111.09
Ge(1)Sn(3)	2.5917	Sn(1)Ge(1)Sn(4)	109.08
Ge(1)Sn(4)	2.5912	Sn(2)Ge(1)Sn(3)	107.59
		Sn(2)Ge(1)Sn(4)	109.91
		Sn(3)Ge(1)Sn(4)	108.29

[a] Distances in Angstroms and bond angles in degrees.

structural parameters obtained from a single-crystal structure determination are listed in Table 4. Details on the structural determination will be provided in a subsequent publication.[34] From these data, an average Ge−Sn bond length of 2.5934 Å may be calculated, which compares very favorably with the predicted value 2.5680 Å for a $Ge(SnH_3)_4$ analogue. As shown in Table 3, similar excellent agreement is also found between the known bond lengths in elemental α-Sn and diamond-cubic Ge and our ab initio calculations. Again, the ∼1% underestimation in the theoretical values is typical of the local density approximation (LDA) used in our calculations. Future work in this system will focus on the synthesis of cluster compounds containing the $Sn(Sn)_4$ and $Sn(Ge)_4$ tetahedral cores to obtain experimental deviations from ideal behavior for this intriguing alloy system.

In contrast to the paucity of bond length data for Sn−Ge and Si−Ge clusters, reliable information about carbide clusters based on Si−C and Ge−C is readily available.[35−39] Bond lengths such as C−C, Si−C, C−Si, Ge−C, and C−Ge are obtained from the crystal

(28) Xiong, J. Z.; Jiang, D.; Dixon, C. E.; Baines, K. M.; Sham, T. K. *Can. J. Chem.* **1996**, *74*, 2229.
(29) Mallela, S. P.; Hill, S.; Geanangel, R. A. *Inorg. Chem.* **1997**, *36*, 6247.
(30) Whittaker, S. M., Brun, M.-C.; Cervantes-Lee, F.; Pannell, K. H. *J. Organomet. Chem.* **1995**, *499*, 247.
(31) This was carried out by the addition 0.1 g of GeH_4 (1.3 mmol) to 1.0 g of Me_3SnNMe_2 (5 mmol) at −196 °C. The mixture was warmed to room temperature and stirred for 24 h. The volatiles were identified as $HNMe_2$ and small amounts of GeH_4 by gas-phase IR and were removed at room temperature in vacuo. The white solid was recrystallized from a saturated toluene solution at −20 °C and the purity was confirmed by matching the IR, powder XRD, ^{1}H NMR, and melting point with the published values. This represents a simpler alternative than the multistepped reaction, hydrolysis, and separation procedure required with the reaction of Me_3SnLi and $GeCl_4$ in THF. See Leites, L. A.; Bukalov, S. S.; Garbuzova, I. A.; Lee, V. Ya.; Baskir, E. G.; Egorov, M. P.; Nefedov, O. M. *J. Organomet. Chem.* **1999**, *588*, 60−61. Larger crystals, suitable for single-crystal XRD, were grown by subliming the pure powder in a sealed quartz tube held at 100 °C on one end and room temperature on the other. In contrast, subliming the microcrystalline powders at 135 °C in vacuo yields only microcrystalline powders.
(32) Dinnebier, R. E.; Bernatowicz, P.; Helluy, X.; Sebald, A.; Wunschel, M.; Fitch, A.; Smaalen, S. *Acta Crystallogr.* **2002**, *B58*, 52−61.
(33) Wrackmeyer, B.; Bernatowicz, P. *Magn. Reson. Chem.* **1999**, *37*, 418−420.
(34) Bauer, M.; Kouvetakis, J. *Acta Crystal. C* (in preparation).
(35) Kouvetakis, J.; Nesting, D.; Smith, D. J. *Chem. Mater.* **1998**, *10*, 2935.
(36) Hencher, J. L.; Mustoe, F. J. *Can. J. Chem.* **1975**, *53*, 23.
(37) Hager, R.; Steigelmann, O.; Muller, G.; Schmidbaur, H.; Robertson, H. E.; Rankin, D. W. H. *Angew. Chem., Int. Ed.* **1990**, *29*, 201.

structures of the compounds $(CH_3)_4C$, $Si(CH_3)_4$, $C(SiH_3)_4$, $Ge(CH_3)_4$, and $C(GeH_3)_4$, respectively.[35−39] A comparison between these experimental data and the theoretical predictions for Si−C and Ge−C based clusters is therefore also included in Table 3. As can be seen, the observed isotropic bond lengths b_{CC}, b_{SiSi}, and b_{GeGe} are all consistently reproduced by the ab initio calculations to within an accuracy of about 2%. The slight underestimation obtained therefore systematically reduces the isotropic bond length (b_{iso}) averages viz a viz experiment for Si−C and Ge−C by a comparable amount. As mentioned earlier, the anisotropic bond lengths are very similar in all systems considered in the present study. We observe that while the ordering (e.g., $b_{SiC} > b_{CSi}$ and $b_{CGe} > b_{GeC}$) is reproduced by our ab initio calculations, the magnitude of the difference $|b_{AB} - b_{BA}|$ is slightly overestimated in the Si−C system. Nevertheless, as can be seen from the data in Table 3, the magnitude and sign of the deviations from ideal bonding in clusters, as measured by δb, are in very good agreement with experiment. In the case of SiC, for which experimental data is available for the alloy, the predicted deviations computed for the solid state agree very well with experiment. It is remarkable that, in this system, and for Si−Ge, the deviations from Vegard behavior are essentially the same in the clusters and the solids. This lends support to our assertion that the mechanism responsible for these deviations is essentially present at the molecular level in group IV tetrahedral systems.

An intriguing possibility suggested by our findings is that Vergard's Law violations (at least in the class of materials studied here) do not have a "solid state" origin. Yet most current theoretical attempts at a systematic treatment of the phenomenon are couched within the conceptual framework of an extended periodic system. It is therefore instructive to compare the present ab initio predictions with various simplified solid-state models for the deviations from linearity. Departures from Vegard's Law are most often expressed as a quadratic correction of the form

$$a(x) = a_B(1 - x) + a_A x + \theta x(1 - x) \qquad (2)$$

where θ is the so-called bowing parameter, usually assumed constant. A simple expression for the composition dependence of the bowing function was derived by Fournet.[10] For an A_xB_{1-x} alloy (e.g., composed of elements "A" and "B") it takes the form[24]

$$\theta(x) = (a_B - a_A)\left\{\frac{\lambda_B}{\lambda_A} + F - 1\right\}\left\{(1 - x) + x\frac{\lambda_B}{\lambda_A}\right\}^{-1} \qquad (3)$$

where a_k and B_k are the lattice constant ($a_B > a_A$ assumed) and bulk modulus of the constituent systems $\{k = A,B\}$, respectively, and $\lambda_k = a_k B_k$. The parameter F is a measure of the deviation of the solid solution from a normal random distribution ($F = 0$), but it is difficult to precisely define and compute and is therefore most often used as a fitting parameter. Using the experimental parameters quoted earlier (section III), we find $\lambda_C = 1580$ Å·GPa, $\lambda_{Si} = 553.8$ Å·GPa, $\lambda_{Ge} = 440.5$ Å·GPa, and $\lambda_{Sn} = 279.2$ Å·GPa. From eqs 2 and 3 the departure from Vegard's Law can then be expressed as $\Delta a(x) = \theta(x)/x(1 - x)$ and in the limit of a random $A_{0.50}B_{0.50}$ alloy ($x = 1/2$) we obtain $\Delta a(x = 1/2) = 1/2(a_B - a_A)(\lambda_B - \lambda_A)/(\lambda_B + \lambda_A)$. When the preceding values for λ_k are used, this yields (at $x = 1/2$) $\Delta a_{SnGe} \approx -0.09$ Å, $\Delta a_{GeSi} \approx -0.01$ Å, $\Delta a_{GeC} \approx -0.59$ Å, and $\Delta a_{SiC} \approx -0.45$ Å. A comparison of these values with available experimental data and ab initio predictions indicates that the Fournet formula does not capture the observed Vegard's Law deviations, which in terms of a lattice constant difference are, from Table 3, $\Delta a_{SnGe} = +0.0104$ Å, $\Delta a_{GeSi} = -0.0013$ Å, $\Delta a_{SiC} = -0.1663$ Å, and $\Delta a_{GeC} = -0.0681$ Å. In all four cases considered above, the deviations are found to be too large, and for SnGe the sign is incorrectly predicted. The ordering with respect to magnitude ($|\delta a_{SiC}| > |\Delta a_{GeC}| > |\Delta a_{SnGe}| > |\Delta a_{GeSi}|$) is also not qualitatively described, although the Fournet formula yields that the deviations in the SiGe system are the smallest.

Hafner has recently discussed another systematic approach to the calculation of deviations from Vegard's Law in alloys based on the energy of an electron gas perturbed from the alloy's constituent ionic cores. The latter are represented by simple empty core pseudopotentials and perturbation theory is used to estimate the response of the electron gas to a binary admixture of ion cores.[13] This prescription was applied to a large number of ionic, metallic, and intermetallic alloys in both solid and liquid form and found to yield a reasonable description of the composition dependence of the formation volume in systems exhibiting negative deviations from Vegard's Law. Although data on semiconductor alloys is abundant over a limited composition range comparable to that for the other systems considered, the theory was not applied to group IV alloys. Using the experimental lattice constants, assuming isostructural (zinc blende) lattice structure, and a valence of $Z = 4$, we find, at $x = 1/2$, the following: $\Delta a_{SnGe} \approx +0.0175$ Å, $\Delta a_{GeSi} \approx +0.0014$ Å, $\Delta a_{GeC} \approx +0.152$ Å, and $\Delta a_{GeC} \approx +0.125$ Å. In this case all of the predicted deviations are positive, in disagreement with the data in Table 3. However, the magnitudes are reasonably well predicted and their ordering using this approach $|\Delta a_{GeC}| > |\Delta a_{SiC}| > |\Delta a_{SnGe}| > |\Delta a_{GeSi}|$ is essentially correct, with the exception of the reversal observed for the GeC and SiC systems.

It is evident that neither of these two models for the composition dependence of the lattice constant produces a correct quantitative and systematic description. One possible reason for the failure is that neither approach accounts for the effects of both bond-stretching and bond-bending forces.[40] It has been argued that convex (or concave) behavior in $a(x)$ only occurs in systems in which the former force constants dominate. In this case the polarity of the deviations may be related to the anisotropy in the bond-stretching forces constants associated, for example, the compressibility difference between Sn−Ge bonds in $SnGe_4$ and $GeSn_4$. This notion is corroborated by recent vibrational measurements on $(Me_3Si)_4Sn$ and $(Me_3Sn)_4Si$ molecules,[41] where it is found that the A1 stretch frequencies are significantly

(38) Beagley, B.; Brown, D. P.; Monaghan, J. J. *J. Mol. Struct.* **1969**, *3*, 233.
(39) Campanelli, A. R.; Ramondo, F.; Domenicano, A.; Hargittai, I. *J. Phys. Chem. A* **2001**, *105*, 5933.
(40) Fong, C. Y.; Weber, W.; Philips, J. C. *Phys. Rev. B* **1976**, *14*, 5387.

different (311 cm^{-1} in "Si_4Sn" and 125 cm^{-1} in "Sn_4Si"). A systematic study of bond-bending and bond-stretching forces in the systems described in Table 3 may yield valuable additional insight into the observed deviations from linear composition dependence.

VI. Conclusions

We described the synthesis of a new class of $Ge_{1-x}Sn_x$ alloys achieved using a novel chemical vapor deposition (CVD) synthesis approach based on deuterium-stabilized Sn hydrides precursors**.** A positive deviation from Vegard's Law was found for the experimental lattice constant dependence on composition and this trend was quantitatively confirmed using ab initio simulations based on density functional theory. This unusual compositional variation of the lattice constant was then analyzed by comparing the trends in the SnGe system with those of $Si_{1-x}C_x$ and $Si_{1-x}Ge_x$ group IV alloys for which the deviations from Vegard's Law are known to be negative. To elucidate this intriguing behavior, we re-examined the bonding trends in the solid state from the point of view of molecular clusters sharing the same elemental cores *(*SiC, GeC, SiGe, and SnGe). Our results clearly indicate that the systematic deviations from ideal bonding behavior observed in the extended state solids are already present at the molecular level. These deviations are found to be negative in Si−C, Si−Ge, and Ge−C systems and positive for the newly developed Sn−Ge analogue. The remarkable level of agreement between the ab initio predictions, and all available experimental data for the structure of both the molecular and solid-state forms, is both gratifying and compelling. On the basis of the uniform and systematic computational treatment of the solid-state and molecular forms of Si−C, Si−Ge, and Ge−C, we believe that similar good agreement will be found between SnGe molecules and their corresponding solid-state analogues when additional experimental data become available. Initial comparisons with the $Ge(SnMe_3)_4$ molecular crystals are already very favorable. A detailed study of the charge densities, electronic structure, and energetics of SiC, GeC, SiGe, and SnGe clusters and solids, aimed at uncovering the origin of this intriguing bond length behavior, is currently underway.

Acknowledgment. This work was supported by the National Science Foundation DMR-0221993 and the Army Research Office (ARO) DAAD19-00-1-0471. The computational resources of the Goldwater Materials Visualization Facility in the Center for Solid State Science at Arizona State University are gratefully acknowledged.

CM0300011

(41) Leites, L. A.; Bukalov, S. S.; Garbuzova, I. A.; Lee, V. Ya.; Baskir, E. G.; Egorov, M. P.; Neferov, O. M, *J. Organomet. Chem*. **1999**, *588*, 60.